Impaired IFNγ responsiveness of lung monocyte-derived cells limits immunity to *Mycobacterium tuberculosis*

Weihao Zheng[1], Jason D. Limberis[1], Zachary P. Howard[1], Alex Mohapatra[1], Enzo Takagi[2], Joel D. Ernst[1,*]

1 Division of Experimental Medicine, Department of Medicine, University of California, San Francisco, California, USA

2 Division of Nephrology, Department of Medicine, University of California, San Francisco, California, USA

*Correspondence: joel.ernst@ucsf.edu

Abstract

Lung mononuclear phagocyte (MNP) subsets differ in their ability to restrict *Mycobacterium tuberculosis* (Mtb) during chronic infection, yet the mechanisms driving the differential ability to control Mtb are not well defined. Here, we show that CD11c^{lo} monocyte-derived cells (MNC1), the subset of lung cells that is most permissive for Mtb viability during chronic infection, express lower levels of interferon-gamma (IFNγ) signaling proteins, resulting in reduced responses to IFNγ compared to alveolar macrophages (AM) and monocyte-derived CD11c^{hi} MNC2. We further found that type I IFN signaling suppresses IFNγ-mediated MHC-II expression, resulting in impaired CD4 T cell activation by MNC1 cells. Importantly, prior immunity conferred by contained Mtb infection enhances IFNγ responsiveness of monocyte-derived cells, reducing bacterial burdens in lungs and within MNC subsets. Our findings indicate that heterogeneous IFNγ responsiveness is exploited by Mtb for persistence in vivo. Overcoming or bypassing impaired IFNγ responsiveness may guide the development of more effective TB vaccines and host-directed therapies.

Introduction

Tuberculosis (TB), caused by the respiratory pathogen *Mycobacterium tuberculosis* (Mtb), returned to being the leading cause of death from a single infectious disease worldwide as the COVID-19 pandemic subsided. It is imperative to identify mechanisms of immune protection and pathogenesis in TB to facilitate the development of novel TB vaccines and therapies.

Mtb is known for its ability to evade elimination by immune responses and cause chronic infection[1–3]. Mounting evidence has established that Mtb infects multiple subsets of lung mononuclear phagocytes (MNP), among them, monocyte-derived cells (MNC) serve as the major bacterial reservoir during chronic infection[4–8]. After development of adaptive immune responses, distinct lung MNP subsets differ in Mtb-killing ability. Specifically, alveolar macrophages (AM) have a superior ability to restrict Mtb compared to MNC1 and MNC2 cells [5,6]. Among these MNP subsets, CD11c^{lo} MNC1 is the most Mtb-permissive subset, suggesting that functional heterogeneity of MNP contributes to Mtb persistence in vivo. We previously discovered heterogeneous lysosome function in these MNP subsets and found that in MNC1, lysosome

deficiency is one cell type-specific host mechanism that contributes to Mtb persistence in vivo[5]. Despite this, we know little about the mechanisms of functional heterogeneity that support Mtb survival in distinct lung MNP subsets.

Interferon-gamma (IFNγ) plays a critical role in host defense against Mtb, as evidenced by both human and murine studies[9–13]. Individuals with mutations in genes responsible for IFNγ immunity (e.g., *Ifng*, *Ifngr1*, *Ifngr2*, and *Stat1*) are susceptible to mycobacterial infections, including non-tuberculous mycobacteria and Mtb[9,14]. Studies utilizing knockout mice have demonstrated that both IFNγ and its receptor, IFNGR1, are essential for controlling Mtb infection, suggesting that the host's ability to produce IFNγ or to respond to IFNγ is required for IFNγ-mediated protection against TB[10–12]. Both hematopoietic and nonhematopoietic IFNγ responsiveness are required for Mtb control[12]. Despite these insights, we lack an understanding of myeloid subset-specific IFNγ signaling during Mtb infection. Moreover, strong evidence indicates that the contribution of IFNγ to Mtb control in the lungs may be limited relative to its contribution to control in other tissues[15]. It is also unknown whether distinct lung MNP subsets respond to IFNγ differently during primary Mtb infection, and whether there are interventions that alter IFNγ responsiveness in lung MNP subsets to affect infection outcome. Elucidating cell-specific actions of IFNγ is crucial for a comprehensive understanding of IFNγ-mediated immunity in tuberculosis, to make it more effective.

In this study, we first investigated responses to endogenous and exogenous IFNγ in different MNP subsets isolated from mouse lungs during chronic Mtb infection and found evidence of differential IFNγ responses in distinct lung MNP subsets. Furthermore, compared with AM, Mtb-permissive MNC1 cells are less responsive to IFNγ, while MNC2 cells exhibit intermediate responsiveness to IFNγ. Compared with AM and MNC2 cells, MNC1 cells express less MHC II and have a reduced ability to present Mtb antigens to CD4 T cells, which is partially dependent on Type I IFN signaling. We further found that prior Mtb immunity can improve IFNγ responsiveness of MNC cells, leading to better Mtb control. Our study reveals heterogeneous IFNγ responses in lung mononuclear phagocytes as a mechanism to enable Mtb persistence in vivo, and that targeting IFNγ responsiveness may represent a strategy for developing novel TB therapies.

Results

Differential responses to IFNγ in MNP subsets from *M. tuberculosis*-infected lungs.

To investigate if lung MNP subsets might respond to IFNγ differently during chronic Mtb infection, we first analyzed our bulk RNA-seq data for three flow-sorted lung MNP subsets (AM, CD11c^{lo} MNC1, and CD11c^{hi} MNC2) from mice infected with Mtb for 28 days (GSE220147) (Figure S1)[5]. Gene Ontology (GO) analysis revealed that IFNγ-responsive genes were expressed at significantly lower levels in MNC1 compared to AM or MNC2 (Table S1). We further investigated the expression levels of IFNγ-responsive genes in a published gene list[16,17]. In this analysis, MNC1 cells exhibited decreased expression of IFNγ-responsive genes compared to AM and MNC2 (Figure 1A), suggesting that this lung cell subset responds to IFNγ less effectively. Since IFNγ receptors and downstream regulators/proteins in the pathway dictate the cellular response to IFNγ (Figure 1B), we investigated their expression levels. This revealed that MNC1 had lower mRNA expression of *Ifngr2*, *Stat1*, *Irf1*, *Cxcl9*, and *Nos2* compared to MNC2, while AM expressed

more mRNA *Ifngr2*, *Stat1* and *Cxcl9* than MNC1 (Figure 1C). Using flow cytometry, we confirmed that MNC1 expressed lower levels of IFNGR2, STAT1, and IRF1 proteins, as well as the IFNγ-responsive proteins CXCL9 and NOS2, compared to AM or MNC2 (Figure 1D). IFNGR1 is another key subunit in the receptor complex, but its protein level did not differ in AM, MNC1, and MNC2 (Figure S2). Together, these findings indicate that there are differential signaling and responses to IFNγ in these lung MNP subsets.

MNC1 are deficient in responding to IFNγ ex vivo.

Based on the above findings, we hypothesized that lung MNP subsets isolated from lungs during chronic Mtb infection either differ in their ability to respond to IFNγ, or that differential responses were due to differential exposure to IFNγ, perhaps due to their positioning or access to IFNγ in vivo. To distinguish these two possibilities, we compared responses to ex vivo IFNγ stimulation for lung MNP subsets by flow cytometric analysis of tyrosine phosphorylated STAT1 (pSTAT1), a key early signaling step in IFNγ cell activation. We prepared lung single-cell suspensions from Mtb-infected mice (28 dpi) and treated them with or without IFNγ (Figure 2A). Without IFNγ stimulation, AM and MNC2 showed higher pSTAT1 levels than MNC1, likely reflecting IFNγ stimulation in vivo. With ex vivo IFNγ stimulation, AM, MNC1, and MNC2 exhibited a 5.1-fold, 2.3-fold, and 2.5-fold increase of pSTAT1, respectively (Figure 2B-2C); however, MNC1 still showed a lower pSTAT1 signal than AM or MNC2 (Figure 2B). Interestingly, the difference in IFNγ responsiveness among AM, MNC1, and MNC2 did not depend on the presence of Mtb in individual cells (Figure S3). Moreover, infected AM and infected MNC2 responded to IFNγ better than their bystander counterparts (Figure S3). We also observed a similar phenotype at later time points of Mtb infection (Figure S4).

Since pSTAT1 functions in the nucleus, we used immunofluorescence to quantify nuclear pSTAT1 in sorted mononuclear cells with or without ex vivo IFNγ. In the absence of IFNγ addition, the nuclear pSTAT1 level was similar in cells in all three subsets (Figure 2D). However, after IFNγ stimulation, we observed a lower level of nuclear pSTAT1 in MNC1 cells compared to AM and MNC2, while MNC2 had an intermediate level of nuclear pSTAT1 between that of AM and MNC1 (Figure 2E). Furthermore, in response to IFNγ stimulation, MNC1 showed a lower fold change of nuclear pSTAT1 (1.5-fold) than AM (4.3-fold) or MNC2 (2.4-fold) (Figure 2F). Collectively, these results indicate that responsiveness to IFNγ is impaired in MNC1 compared with AM or MNC2.

MNC1 are impaired for activating Mtb antigen-specific CD4 T cells.

One effect of IFNγ is to upregulate MHC-II, which mediates antigen presentation and CD4 T cell activation[18–20]. Therefore, we hypothesized that MNP subsets that differ in IFNγ responsiveness also differ in MHC-II expression and antigen presentation. GO analysis revealed that mRNAs encoding multiple components of the MHC-II antigen presentation pathway are differentially regulated when comparing AM or MNC2 to MNC1 (Table S2). We found that class II transactivator (CIITA), the master transcription factor for MHC-II expression, and other MHC-II antigen presentation-related genes are underexpressed in MNC1 (Figure 3A). Using flow cytometry, we

122 confirmed that MHC-II and CD74 (the MHC-II invariant chain) are expressed at lower levels in
123 MNC1 cells compared to AM and MNC2 (Figure 3B). Differential MHC-II expression was also
124 observed at 42 dpi and 56 dpi (Figure S5). Next, we sought to determine whether reduced MNC1
125 expression of MHC-II results in poorer antigen presentation to CD4 T cells. To specifically study
126 antigen presentation independently of potential differences in antigen processing, we incubated
127 sorted cells from MNP subsets from Mtb-infected mice with C7 or P25 epitope peptides (from
128 ESAT-6 or Ag85B, respectively), and antigen-specific Th1-polarized C7 or P25 TCR transgenic
129 CD4 T cells, then used IFNγ ELISA as a readout of T cell activation (Figure 3C). Consistent with
130 the levels of expression of MHC II pathway molecules, we observe lower responses by antigen-
131 specific CD4 T cells when stimulated by MNC1 compared with AM or MNC2 (Figure 3D),
132 confirming that MNC1 cells have an impaired ability to present Mtb antigens to CD4 T cells.

133

134 **Type I IFN inhibits MHC-II expression in primary macrophages and lung MNPs**

135 We next investigated the potential mechanisms regulating MHC-II expression in lung MNP
136 subsets. From our bulk RNA-seq data, we found a higher type I IFN signature in MNC1 and MNC2
137 compared to AM (Figure 4A), consistent with results from our prior study[6]. Since type I IFN has
138 been reported to cause down-regulation of IFNGR [21–23], we reasoned that type I IFN might
139 suppress IFNγ-mediated MHC-II upregulation in MNPs/macrophages in Mtb infection. To test this,
140 we differentiated bone marrow-derived macrophages (BMDM) in the presence of IFNγ and/or
141 IFNβ, and quantified MHC-II expression by flow cytometry. As expected, IFNγ significantly
142 increased MHC-II in wild-type (WT) BMDM (Figure 4B). IFN-β alone slightly reduced MHC-II
143 expression and inhibited IFNγ-mediated MHC-II upregulation. Deletion of the type I IFN receptor,
144 *Ifnar1*, completely negated the inhibitory effect of IFNβ on MHC-II expression in BMDM (Figure
145 4C).

146 To further investigate the effect of type I IFN on MHC-II expression on different MNP subsets in
147 vivo, we generated mixed bone marrow chimeric mice (Figure 4D). Irradiated WT recipient mice
148 received WT and *Ifnar1*$^{-/-}$ mixed bone marrow cells. After reconstitution, the mice were infected
149 with Mtb by aerosol and harvested 28 dpi. All *Ifnar1*$^{-/-}$ lung MNP subsets showed higher MHC-II
150 expression compared to the analogous WT subsets (Figure 4E and Figure S6). Together, these
151 results indicate that type I IFN negatively regulates IFNγ-mediated MHC-II expression in BMDM
152 and in lung MNP subsets in vivo in the context of Mtb infection.

153

154 **CoMtb-mediated prior immunity improves IFNγ responsiveness of MNC cells but not AM**

155 Since monocytes and macrophages are functionally reprogrammable, we investigated whether
156 pre-existing immunity alters IFNγ responsiveness of MNP subsets, using the contained Mtb
157 (CoMtb) model[24]. This model is established by intradermal infection of Mtb in the mouse ear,
158 which results in Mtb trafficking to the local draining lymph nodes without bacterial dissemination
159 to other organs, including the lungs.

160 Since MNC cells are derived from monocytes[5,6,25,26], we first asked whether CoMtb regulates IFNγ
161 responsiveness in bone marrow monocytes ex vivo. For this, we established CoMtb for 4-6 weeks
162 (Figure 5A), then harvested bone marrow cells from CoMtb and control mice. Without IFNγ

163 stimulation, we observed higher pSTAT1 in CoMtb bone marrow monocytes compared with
164 control monocytes (Figure 5B). After IFNγ stimulation, CoMtb monocytes showed greater STAT1
165 activation than control monocytes; BMDM from CoMtb mice also exhibited greater pSTAT1 than
166 did BMDM from control mice. These data suggest that CoMtb conditions monocytes and
167 macrophages to improve their IFNγ responsiveness in vivo (Figure 5B-5C).

168 We further investigated the effect of CoMtb on IFNγ responsiveness in lung MNP subsets from
169 mice after subsequent aerosol Mtb infection. Using flow cytometry detection of pSTAT1 to
170 quantitate IFNγ responses, we found that CoMtb improved responses to IFNγ in MNC1 and MNC2
171 cells, but not in AM, (Figure 5D). CoMtb also increased expression of IFNGR2 and the IFNγ-
172 regulated proteins MHC-II and NOS2 (Figure 5B). These results indicate that CoMtb improves
173 IFNγ responsiveness in monocyte-derived cells that traffic to the lungs after aerosol Mtb challenge.

174

175 **CoMtb-mediated control of Mtb in lung monocyte-derived cells requires IFNγ signaling**

176 As indicated by whole lung CFU, we confirmed that CoMtb reduced Mtb burden in the lung after
177 aerosol infection (Figure 6A); we also found that CoMtb reduced the number of total Mtb-infected
178 cells in the lungs and lower bacterial fluorescence intensity (indicative of the per-cell bacterial
179 burden) in the infected cells (Figure 6B-6C). We further found that CoMtb decreased the number
180 of infected AM, MNC1, MNC2, and neutrophils compared to the control (Figure 6D). In addition,
181 the infection frequency was reduced in all subsets when comparing CoMtb mice to control mice
182 (Figure 6E). Moreover, we found that CoMtb reduced Mtb burdens in the myeloid subsets,
183 especially MNC1 and MNC2 (Figure 6F). In line with these results, chimeric mice that received
184 bone marrow from CoMtb mice showed lower lung CFU burdens than mice that received control
185 bone marrow cells (Figure S7). Thus, these findings indicate that improved IFNγ responsiveness
186 can enhance Mtb control in monocyte-derived lung cells.

187 We next sought to determine whether IFNγ responsiveness is required for CoMtb-mediated Mtb
188 control in MNC cells. For this, we generated mixed bone marrow chimeric mice (Figure 6G and
189 Figure S7A). Irradiated WT mice received WT and *Ifngr1*$^{-/-}$ mixed bone marrow cells (1:1). After
190 reconstitution and CoMtb establishment, they were infected with Mtb by aerosol and harvested at
191 28 dpi. This revealed higher bacterial burdens in *Ifngr1*$^{-/-}$ myeloid cells compared to WT myeloid
192 cells from the same chimeric mouse (Figure 6H and Figure S8). Similarly, we observed a higher
193 Mtb burden in *Ifngr1*$^{-/-}$ MNC cells compared to WT counterparts (Figure 6H-6I). However, we did
194 not observe a difference in Mtb burden between WT and *Ifngr1*$^{-/-}$ AM at 28 dpi (Figure 6H),
195 consistent with our data showing that CoMtb plays a minimal role in AM at the later stage of Mtb
196 infection, in contrast to the effect of CoMtb on AM at an early stage of infection[24]. Collectively,
197 these results suggest that CoMtb-mediated prior immunity enhances Mtb control in MNC cells,
198 which depends on IFNγ signaling.

199 **Discussion**

200 The predominant adaptive immune response to Mtb infection in mice, nonhuman primates, and
201 humans is represented by T lymphocytes that produce IFNγ[13,18,27–33], yet immunity is often
202 incomplete[1]. Multiple observations indicate that, while IFNγ may be produced in abundant
203 amounts, cellular responses to IFNγ are attenuated during Mtb infection. For example, cultured

204 human and mouse macrophages infected with Mtb are defective in responding to IFNγ through
205 multiple mechanisms that impact macrophage signaling. These mechanisms include prolonged
206 TLR2 signaling initiated by Mtb lipoproteins and other cell wall components[34–39], and inhibition of
207 macrophage responses to IFNγ by IL-6 [40]. Notably, these mechanisms inhibit IFNγ-responsive
208 gene expression at one or more steps downstream of STAT1 activation and function[41,42].
209 However, the in vivo relevance of these mechanisms of inhibition of macrophage responses to
210 IFNγ has not been established.

211 Further evidence that responses to IFNγ are affected by Mtb infection is provided by the finding
212 that in mice, the contribution of IFNγ to T cell control of Mtb in the lungs is less than that in the
213 spleen[15]. While this evidence aligns with the hypothesis that other T cell effector mechanisms are
214 more relevant in the lungs, it is also consistent with a model in which certain lung macrophage
215 populations are less responsive to the effects of IFNγ, as the lungs are the predominant site of
216 Mtb infection and bacterial burden. Additional evidence that cellular responses to IFNγ are
217 attenuated in the lungs was provided by the finding that increasing production of IFNγ by T cells
218 did not provide additional control of Mtb[15].

219 While it is widely acknowledged that Mtb resides in macrophages in the lungs, we and others
220 have determined that Mtb resides in cells representing multiple macrophage subsets in the lungs[4–
221 8,19,43–46], indicating that different mechanisms may determine Mtb killing or survival in distinct cell
222 types. Moreover, the distribution of Mtb in distinct macrophage subsets differs with the stage of
223 infection. In early infection prior to development of adaptive T cell responses, Mtb is found
224 predominantly in yolk sac-derived AM[43–45], while after adaptive T lymphocytes are primed and
225 recruited to the lungs, Mtb is found in monocyte-derived macrophages that are derived from
226 monocytes produced in the bone marrow[4–8]. Adaptive T cells contribute to determining the fate
227 and state of Mtb in distinct lung mononuclear cell subsets, and T cells have a greater impact on
228 suppressing Mtb in AM than in recruited mononuclear cells in the lungs[4].

229 Here, we identified a previously undefined mechanism that contributes to the suboptimal efficacy
230 of IFNγ in immunity to Mtb. Using an unbiased initial approach, bulk RNA sequencing of flow-
231 sorted mononuclear-macrophage cell subsets (AM and two subsets of lung monocyte-derived
232 cells), we detected evidence that one of the monocyte-derived cell subsets (termed MNC1)
233 expresses lower levels of transcripts for IFNγ-responsive genes when compared with AM or the
234 other monocyte-derived cell subset (MNC2). Since this could have reflected differential exposure
235 of these cells to IFNγ in vivo, we treated lung cell suspensions ex vivo with IFNγ and found that
236 MNC1 cells are less responsive to IFNγ as manifested by reduced tyrosine phosphorylation of
237 STAT1. We also found that at the levels of mRNA and cell surface expression, MNC1 cells
238 express lower levels of the IFNγ receptor subunit, IFNGR2, and other key signaling molecules in
239 the response to IFNγ, including STAT1 and IRF1. These results indicate that in MNC1 cells,
240 defective responses to IFNγ are associated with reduced expression of the proximal signaling
241 machinery required for cell responses to IFNγ, and this results in reduced responses to IFNγ in
242 these cells. Notably, we have previously reported that MNC1 cells harbor more viable Mtb per cell
243 than do AM, MNC2 cells, or neutrophils[5], indicating that impaired IFNγ responsiveness contributes
244 to Mtb permissiveness.

245 Although we have not yet fully identified the regulatory pathway(s) responsible for reduced
246 expression of the signaling molecules required for responses to IFNγ, we found that type I

interferon signaling contributes to reduced expression of MHC II, one of the important downstream effectors of IFNγ in myeloid and other cells. Moreover, we found that the responsiveness of MNC1 cells to IFNγ can be modulated: we determined that pre-existing immunity to Mtb established by low-level extrapulmonary infection modifies bone marrow precursors of MNC1 and MNC2 cells to improve their responses to IFNγ and improve their ability to control Mtb. In this manner, our results are consistent with trained immunity[47], since we found that the impact of CoMtb on myeloid cells influenced ex vivo responses to IFNγ and that transfer of bone marrow cells from mice with CoMtb improved control of Mtb after aerosol challenge. Together, these results indicate that modulation of MNC1 cells can be achieved, suggesting that this may be an especially valuable target for host-directed therapies for TB.

We also note that the same cell subset (MNC1) that is deficient in responses to IFNγ is the same subset that we previously reported as being deficient in lysosome biogenesis. Since there are no known connections between IFNγ responsiveness and lysosome biogenesis, our results are most consistent with a model in which both pathways are regulated by a common developmental pathway during differentiation of bone marrow monocytes into monocyte-derived macrophages in the lungs of Mtb-infected mice. Further investigation of the differentiation or maturation of monocytes recruited to the lungs in response to Mtb will be needed for a more thorough understanding of the determinants of cell responsiveness to IFNγ and of lysosome biogenesis.

A shortcoming of the studies reported here is that they only involved studies in mice. Since the cell populations we studied are rare in the lungs of uninfected mice, and since isolation of macrophages from the lung parenchyma of humans infected with Mtb is limited by the rarity of appropriate samples in proximity to facilities for the procedures required, considerable dedicated efforts will be required to determine which of our findings are applicable to humans. Nevertheless, our results provide further mechanistic insight into the potential functional significance of macrophage heterogeneity in the lungs in the context of Mtb infection and should drive further investigation of methods to optimally develop and test host-directed therapies for TB.

Acknowledgments

We thank Lucas Chen, Michael Kwon, and Kelley Martinez for technical assistance. This work was supported by NIH grants R01 AI051242 (J.D.E.), U01 AI166309 (J.D.E.), P30 AI168440/R25 AI147375 (W.Z. and A.M.), T32 HL007185 (A.M.), F32 HL162424 (A.M.), and F31 AI172360 (Z.P.H.). The funders had no role in study design, data collection, interpretation, or the decision to submit the work for publication.

Author contributions

Conceptualization, W.Z. and J.D.E.; methodology, W.Z., J.D.L., and Z.P.H.; investigation, W.Z., J.L., Z.P.H., and A.M.; resources: E.T.; writing—original draft, W.Z. and J.D.E.; writing—review & editing, W.Z. and J.D.E.; funding acquisition, W.Z., Z.P.H., A.M., and J.D.E.; supervision, J.D.E.

287 **Methods**

288 **Mice**

289 8-12-week-old C57BL/6 (Strain #:000664), *Ifnar1*$^{-/-}$ (Strain #:028288) and *Ifngr1*$^{-/-}$ (Strain
290 #:003288) mice were obtained from Jackson Laboratory. Mice infected with Mtb were housed in
291 the Animal Biosafety Level 3 facility. All animal experiments were approved by the Institutional
292 Animal Care and Use Committee of the University of California, San Francisco.
293

294 **Bacterial strains, growth, and aerosol infection**

295 Mtb H37Rv was transformed with pMV261::ZsGreen and cultured in Middlebrook 7H9 medium
296 (BD) supplemented with 10% (v/v) ADC (albumin, dextrose, catalase), 0.05 % Tween 80, 0.2 %
297 glycerol, and 50 µg/ml kanamycin[5]. Mice were infected with H37Rv or pMV261::ZsGreen via
298 aerosol using a Glas-Col inhalation exposure unit, as previously described[5,6,25,46]. Mid-log
299 cultures were centrifuged at 800g for 8 min. Clump-free cultures were transferred and diluted,
300 and 5 mL of inoculum was added to the nebulizer. The target dose was 100 CFU/mouse.
301 Infection dose was determined by plating lung homogenates 24 hours post-infection on 7H11
302 agar plates. CFUs were counted after incubation of plates at 37°C for 3 weeks.
303

304 **Lung homogenate preparation, flow cytometry, and cell sorting**

305 Lung homogenates were prepared as described previously[5,6]. Lungs were perfused with 10 mL
306 of PBS/2 mM EDTA via the right ventricle immediately after euthanasia. Lungs were processed
307 with a gentleMACS dissociator (Miltenyi, lung program 1), and digested in 4 mL of RPMI-
308 1640/5% HI-FBS containing 1 mg/mL collagenase D (Sigma-Aldrich) and 50 µg/mL DNase I
309 (Sigma-Aldrich) for 30 min at 37 °C. Digested lung tissues were further dissociated with the
310 gentleMACS dissociator (lung program 2) and then passed through a 70-µm cell strainer. Red
311 blood cells were lysed with 3 mL ACK lysis buffer (Gibco) for 3 min and washed twice with
312 RPMI-1640/5% HI-FBS.
313

314 For staining of surface antigens, cells were washed with PBS, then stained with 1:200 Zombie
315 Aqua Fixable Viability Dye (BioLegend, 423101) and 1:100 anti-CD16/32 (clone 2.4G2; Fc
316 receptor blockade) for 15 min at 4°C. After washing with PBS, cells were stained with flow
317 antibodies from Table S3 in 1:1 PBS/Brilliant Stain Buffer (BD, 566349) for 30 min at 4°C. Samples
318 were washed twice with PBS, then fixed overnight in 1% paraformaldehyde (PFA)/PBS. For cell
319 sorting, cells were washed and resuspended in FACS buffer (PBS, 2% HI-FBS (v/v), 2 mM EDTA
320), and sorting was done using the BSL3 Sony MAC900 cell sorter.

321 For intracellular staining, cells were fixed and permeabilized using BD Fixation/Permeabilization
322 Kit for 20 min at 4°C after surface staining, then washed and incubated with antibodies diluted in
323 1x BD Perm Wash/0.5% FBS for 30 min at RT. For IRF1, 0.1% Triton X-100/PBS was used for
324 permeabilization. Samples were washed and acquired using an Aurora spectral flow cytometer
325 (Cytek Biosciences) or Sony MA900.

326

327

328 **Ex vivo IFNγ stimulation for pSTAT1 flow cytometry**

329 10^6 cells per lung were stained with Zombie Aqua Fixable Viability Dye as described above at 4°C
330 for 15 min. Samples were washed once with RPMI-1640/5% HI-FBS, then stimulated with 100 µL
331 of 20ng/mL IFNγ (final concentration) (Biolegend, 575304) in media at 37°C for 15 min. Untreated
332 samples were kept at 4°C. Samples were then mixed with 100 µL of 4% PFA/PBS and fixed at
333 room temperature (RT) for 15 min. Cells were washed once with PBS, followed by
334 permeabilization with 180 µL of cold methanol at 4°C for 12 min. After this, samples were washed
335 twice and incubated with 50 µL of 1:50 anti-CD16/32 in PBS for 5 min, followed by the addition of
336 antibodies, including AF647-pSTAT1 (Cell Signaling Technology, 8009S), diluted in 50 µL of
337 Brilliant Stain Buffer and incubated for 30 min at RT. After washing twice with PBS, samples were
338 resuspended in 1% PFA/PBS.

339 **Immunofluorescence**

340 Lung cell subsets were sorted from mice infected with H37Rv-ZsGreen. 40,000 cells/well were
341 seeded into 8-well Nunc Lab-Tek chamber slides (Thermo Scientific, 177445), and rested in a cell
342 incubator for 1 h. Media were replaced with 100 µL of RPMI-1640/5% HI-FBS with or without
343 20ng/mL IFNγ, and cells were incubated for 15min at 37°C. Immunofluorescence was performed
344 as previously described with slight modifications[5,48,49]. Media were removed and cells were fixed
345 immediately with 4% PFA for 30min. Slides were immersed in 1% PFA/PBS and transferred to
346 BSL2. Cells were washed twice with 200 µL PBS, followed by permeabilization with 200 µL of ice-
347 cold methanol for 10 min at 4°C, and then washed 3 times with PBS. Samples were blocked with
348 5% goat serum/PBS for 30 min at RT, then incubated with 100 µL of pStat1 (Tyr701) Rabbit mAb
349 (Cell Signaling Technology, 9167S, 1:200 diluted in 5% goat serum/PBS) for 2 h at RT. Then cells
350 were washed three times with PBS and stained with 1:1000 Goat anti-Rabbit IgG AF647
351 (Invitrogen, A-21244) for 1 h at RT. Samples were washed three times with PBS and mounted
352 with ProLong Diamond Antifade Mountant with DAPI.

353 **T cell and MNP coculture**

354 T cell and MNP coculture were done as described previously[20,50]. ZsGreen$^-$ Lung MNP subsets
355 (AM, MNC1 and MNC2) were sorted from mice infected with H37Rv-ZsGreen. 10,000/well of MNP
356 were cultured with P25TCR-Tg or C7TCR-Tg Th1 effector cells (200,000/well) in the presence of
357 10 µg/mL Ag85B peptide 25. Supernatants were collected at day 4 and assayed for IFNγ by
358 ELISA.

359 **BMDM differentiation**

360 BMDM were differentiated as described previously[5]. Briefly, bone marrow cells were cultured in
361 BMDM media [DMEM (Gibco, 11965092), 10% heat-inactivated FBS (HI-FBS), and 20 ng/ml
362 recombinant murine M-CSF (PeproTech)] for 6-7 days, and media change was done at day 3.
363 For differentiation with interferon, BMDM media containing 50 pg/mL of IFNγ (Biolegend, 575304)
364 or IFN-β (Sino Biological, 50708-MCCH) were used. At day 6-7, cells were washed twice with
365 PBS and incubated with cold PBS/2mM EDTA for 5 min, then harvested by pipetting.

366

367

368 **Generation of bone marrow chimeras**

369 Bone marrow chimeras were generated as described previously[12]. Bone marrow cells were
370 harvested from the femurs and tibias of donor mice. After ACK lysis, cells were washed once with
371 DMEM/10% HI-FBS, once with PBS, then filtered with a 70 µm strainer. Recipient mice were
372 irradiated with a Precision X-Rad320 X-Ray irradiator using a dose of 10 Gy. Within 24h post-
373 irradiation, 6×10^6 total bone marrow cells were retro-orbitally injected into recipient mice using a
374 28G insulin syringe. Irradiated mice were given TMP-SMX antibiotic (Sulfamethoxazole and
375 Trimethoprim Oral Suspension, 200 mg/40 mg per 5 mL, use 7.5 mL per 293 mL drinking water)
376 for 3 weeks. Mice were allowed to reconstitute for at least 6-8 weeks.

377 **Establishment of CoMtb**

378 CoMtb was established as described previously[24]. Briefly, mice were anesthetized with isoflurane.
379 1×10^4 CFU of Mtb H37Rv were injected intradermally into the base of the ear in 10 µL PBS using
380 a 31 G insulin syringe.

381 **RNA sequencing and data analysis**
382 Analysis of the RNA-sequencing dataset GSE220147 was performed as described previously[5].

383 **Statistical analysis**

384 Results are expressed as mean and standard error. Quantification of MFI from
385 immunofluorescence images was done using ImageJ, and the data are background-subtracted.
386 MFI data shown for lung subsets were net MFI after subtracting the background MFI of the FMO
387 control. Statistical analysis and p-values are stated in the figure legends and indicated in the
388 figures, respectively. $P < 0.05$ is considered significant.

389 **References**

390 1. Ernst, J.D. (2018). Mechanisms of M. tuberculosis Immune Evasion as Challenges to TB
391 Vaccine Design. Cell Host Microbe *24*, 34–42. https://doi.org/10.1016/j.chom.2018.06.004.
392 2. Chandra, P., Grigsby, S.J., and Philips, J.A. (2022). Immune evasion and provocation by
393 Mycobacterium tuberculosis. Nat Rev Microbiol *20*, 750–766. https://doi.org/10.1038/s41579-
394 022-00763-4.
395 3. Lefrançais, E., Hudrisier, D., Neyrolles, O., Behar, S.M., and Ernst, J.D. (2025). Finding and
396 filling the knowledge gaps in mechanisms of T cell-mediated TB immunity to inform vaccine
397 design. Nat Rev Immunol. https://doi.org/10.1038/s41577-025-01192-z.
398 4. Lai, R., Williams, T., Rakib, T., Lee, J., and Behar, S.M. (2024). Heterogeneity in lung
399 macrophage control of Mycobacterium tuberculosis is modulated by T cells. Nat Commun *15*,
400 5710. https://doi.org/10.1038/s41467-024-48515-7.
401 5. Zheng, W., Chang, I.-C., Limberis, J., Budzik, J.M., Zha, B.S., Howard, Z., Chen, L., and Ernst,
402 J.D. (2024). Mycobacterium tuberculosis resides in lysosome-poor monocyte-derived lung
403 cells during chronic infection. PLoS Pathog *20*, e1012205.
404 https://doi.org/10.1371/journal.ppat.1012205.
405 6. Zheng, W., Borja, M., Dorman, L.C., Liu, J., Zhou, A., Seng, A., Arjyal, R., Sunshine, S.,
406 Nalyvayko, A., Pisco, A.O., et al. (2025). Single-cell analysis reveals Mycobacterium
407 tuberculosis ESX-1-mediated accumulation of permissive macrophages in infected mouse
408 lungs. Sci Adv *11*, eadq8158. https://doi.org/10.1126/sciadv.adq8158.
409 7. Lee, J., Boyce, S., Powers, J., Baer, C., Sassetti, C.M., and Behar, S.M. (2020). CD11cHi
410 monocyte-derived macrophages are a major cellular compartment infected by Mycobacterium
411 tuberculosis. PLoS Pathog *16*, e1008621. https://doi.org/10.1371/journal.ppat.1008621.

8. Wolf, A.J., Linas, B., Trevejo-Nuñez, G.J., Kincaid, E., Tamura, T., Takatsu, K., and Ernst, J.D. (2007). Mycobacterium tuberculosis infects dendritic cells with high frequency and impairs their function in vivo. J Immunol *179*, 2509–2519. https://doi.org/10.4049/jimmunol.179.4.2509.
9. Casanova, J.-L., MacMicking, J.D., and Nathan, C.F. (2024). Interferon-γ and infectious diseases: Lessons and prospects. Science *384*, eadl2016. https://doi.org/10.1126/science.adl2016.
10. Flynn, J.L., Chan, J., Triebold, K.J., Dalton, D.K., Stewart, T.A., and Bloom, B.R. (1993). An essential role for interferon gamma in resistance to Mycobacterium tuberculosis infection. J Exp Med *178*, 2249–2254. https://doi.org/10.1084/jem.178.6.2249.
11. Cooper, A.M., Dalton, D.K., Stewart, T.A., Griffin, J.P., Russell, D.G., and Orme, I.M. (1993). Disseminated tuberculosis in interferon gamma gene-disrupted mice. J Exp Med *178*, 2243–2247. https://doi.org/10.1084/jem.178.6.2243.
12. Desvignes, L., and Ernst, J.D. (2009). Interferon-gamma-responsive nonhematopoietic cells regulate the immune response to Mycobacterium tuberculosis. Immunity *31*, 974–985. https://doi.org/10.1016/j.immuni.2009.10.007.
13. Maciag, K., Plumlee, C.R., Cohen, S.B., Gern, B.H., and Urdahl, K.B. (2024). Reappraising the Role of T Cell-Derived IFN-γ in Restriction of Mycobacterium tuberculosis in the Murine Lung. J Immunol *213*, 339–346. https://doi.org/10.4049/jimmunol.2400145.
14. Bustamante, J., Boisson-Dupuis, S., Abel, L., and Casanova, J.-L. (2014). Mendelian susceptibility to mycobacterial disease: genetic, immunological, and clinical features of inborn errors of IFN-γ immunity. Semin Immunol *26*, 454–470. https://doi.org/10.1016/j.smim.2014.09.008.
15. Sakai, S., Kauffman, K.D., Sallin, M.A., Sharpe, A.H., Young, H.A., Ganusov, V.V., and Barber, D.L. (2016). CD4 T Cell-Derived IFN-γ Plays a Minimal Role in Control of Pulmonary Mycobacterium tuberculosis Infection and Must Be Actively Repressed by PD-1 to Prevent Lethal Disease. PLoS Pathog *12*, e1005667. https://doi.org/10.1371/journal.ppat.1005667.
16. Kotov, D.I., Lee, O.V., Fattinger, S.A., Langner, C.A., Guillen, J.V., Peters, J.M., Moon, A., Burd, E.M., Witt, K.C., Stetson, D.B., et al. (2023). Early cellular mechanisms of type I interferon-driven susceptibility to tuberculosis. Cell *186*, 5536-5553.e22. https://doi.org/10.1016/j.cell.2023.11.002.
17. Melo-Silva, C.R., Roman, M.I., Knudson, C.J., Tang, L., Xu, R.-H., Tassetto, M., Dolan, P., Andino, R., and Sigal, L.J. (2022). Interferon partly dictates a divergent transcriptional response in poxvirus-infected and bystander inflammatory monocytes. Cell Rep *41*, 111676. https://doi.org/10.1016/j.celrep.2022.111676.
18. Mogues, T., Goodrich, M.E., Ryan, L., LaCourse, R., and North, R.J. (2001). The relative importance of T cell subsets in immunity and immunopathology of airborne Mycobacterium tuberculosis infection in mice. J Exp Med *193*, 271–280. https://doi.org/10.1084/jem.193.3.271.
19. Srivastava, S., and Ernst, J.D. (2013). Cutting edge: Direct recognition of infected cells by CD4 T cells is required for control of intracellular Mycobacterium tuberculosis in vivo. J Immunol *191*, 1016–1020. https://doi.org/10.4049/jimmunol.1301236.
20. Srivastava, S., and Ernst, J.D. (2014). Cell-to-cell transfer of M. tuberculosis antigens optimizes CD4 T cell priming. Cell Host Microbe *15*, 741–752. https://doi.org/10.1016/j.chom.2014.05.007.
21. Eshleman, E.M., Delgado, C., Kearney, S.J., Friedman, R.S., and Lenz, L.L. (2017). Down regulation of macrophage IFNGR1 exacerbates systemic L. monocytogenes infection. PLoS Pathog *13*, e1006388. https://doi.org/10.1371/journal.ppat.1006388.
22. Kearney, S.J., Delgado, C., Eshleman, E.M., Hill, K.K., O'Connor, B.P., and Lenz, L.L. (2013). Type I IFNs downregulate myeloid cell IFN-γ receptor by inducing recruitment of an early

growth response 3/NGFI-A binding protein 1 complex that silences ifngr1 transcription. J Immunol *191*, 3384–3392. https://doi.org/10.4049/jimmunol.1203510.

23. Rayamajhi, M., Humann, J., Penheiter, K., Andreasen, K., and Lenz, L.L. (2010). Induction of IFN-alphabeta enables Listeria monocytogenes to suppress macrophage activation by IFN-gamma. J Exp Med *207*, 327–337. https://doi.org/10.1084/jem.20091746.
24. Nemeth, J., Olson, G.S., Rothchild, A.C., Jahn, A.N., Mai, D., Duffy, F.J., Delahaye, J.L., Srivatsan, S., Plumlee, C.R., Urdahl, K.B., et al. (2020). Contained Mycobacterium tuberculosis infection induces concomitant and heterologous protection. PLoS Pathog *16*, e1008655. https://doi.org/10.1371/journal.ppat.1008655.
25. Mohapatra, A., Norris, B.A., Howard, Z., and Ernst, J.D. (2025). CCR2 recruits monocytes to the lung, while CX3CR1 modulates positioning of CD11cpos cells in the lymph node during pulmonary tuberculosis. mBio, e0123725. https://doi.org/10.1128/mbio.01237-25.
26. Norris, B.A., and Ernst, J.D. (2018). Mononuclear cell dynamics in M. tuberculosis infection provide opportunities for therapeutic intervention. PLoS Pathog *14*, e1007154. https://doi.org/10.1371/journal.ppat.1007154.
27. Green, A.M., Difazio, R., and Flynn, J.L. (2013). IFN-γ from CD4 T cells is essential for host survival and enhances CD8 T cell function during Mycobacterium tuberculosis infection. J Immunol *190*, 270–277. https://doi.org/10.4049/jimmunol.1200061.
28. Leveton, C., Barnass, S., Champion, B., Lucas, S., De Souza, B., Nicol, M., Banerjee, D., and Rook, G. (1989). T-cell-mediated protection of mice against virulent Mycobacterium tuberculosis. Infect Immun *57*, 390–395. https://doi.org/10.1128/iai.57.2.390-395.1989.
29. Müller, I., Cobbold, S.P., Waldmann, H., and Kaufmann, S.H. (1987). Impaired resistance to Mycobacterium tuberculosis infection after selective in vivo depletion of L3T4+ and Lyt-2+ T cells. Infect Immun *55*, 2037–2041. https://doi.org/10.1128/iai.55.9.2037-2041.1987.
30. Lin, P.L., Rutledge, T., Green, A.M., Bigbee, M., Fuhrman, C., Klein, E., and Flynn, J.L. (2012). CD4 T cell depletion exacerbates acute Mycobacterium tuberculosis while reactivation of latent infection is dependent on severity of tissue depletion in cynomolgus macaques. AIDS Res Hum Retroviruses *28*, 1693–1702. https://doi.org/10.1089/AID.2012.0028.
31. Yao, S., Huang, D., Chen, C.Y., Halliday, L., Wang, R.C., and Chen, Z.W. (2014). CD4+ T cells contain early extrapulmonary tuberculosis (TB) dissemination and rapid TB progression and sustain multieffector functions of CD8+ T and CD3- lymphocytes: mechanisms of CD4+ T cell immunity. J Immunol *192*, 2120–2132. https://doi.org/10.4049/jimmunol.1301373.
32. Kwan, C.K., and Ernst, J.D. (2011). HIV and tuberculosis: a deadly human syndemic. Clin Microbiol Rev *24*, 351–376. https://doi.org/10.1128/CMR.00042-10.
33. Mayer-Barber, K.D., and Barber, D.L. (2015). Innate and Adaptive Cellular Immune Responses to Mycobacterium tuberculosis Infection. Cold Spring Harb Perspect Med *5*, a018424. https://doi.org/10.1101/cshperspect.a018424.
34. Pai, R.K., Pennini, M.E., Tobian, A.A.R., Canaday, D.H., Boom, W.H., and Harding, C.V. (2004). Prolonged toll-like receptor signaling by Mycobacterium tuberculosis and its 19-kilodalton lipoprotein inhibits gamma interferon-induced regulation of selected genes in macrophages. Infect Immun *72*, 6603–6614. https://doi.org/10.1128/IAI.72.11.6603-6614.2004.
35. Gehring, A.J., Rojas, R.E., Canaday, D.H., Lakey, D.L., Harding, C.V., and Boom, W.H. (2003). The Mycobacterium tuberculosis 19-kilodalton lipoprotein inhibits gamma interferon-regulated HLA-DR and Fc gamma R1 on human macrophages through Toll-like receptor 2. Infect Immun *71*, 4487–4497. https://doi.org/10.1128/IAI.71.8.4487-4497.2003.
36. Kincaid, E.Z., Wolf, A.J., Desvignes, L., Mahapatra, S., Crick, D.C., Brennan, P.J., Pavelka, M.S., and Ernst, J.D. (2007). Codominance of TLR2-dependent and TLR2-independent modulation of MHC class II in Mycobacterium tuberculosis infection in vivo. J Immunol *179*, 3187–3195. https://doi.org/10.4049/jimmunol.179.5.3187.

37. Fortune, S.M., Solache, A., Jaeger, A., Hill, P.J., Belisle, J.T., Bloom, B.R., Rubin, E.J., and Ernst, J.D. (2004). Mycobacterium tuberculosis inhibits macrophage responses to IFN-gamma through myeloid differentiation factor 88-dependent and -independent mechanisms. J Immunol *172*, 6272–6280. https://doi.org/10.4049/jimmunol.172.10.6272.
38. Banaiee, N., Kincaid, E.Z., Buchwald, U., Jacobs, W.R., and Ernst, J.D. (2006). Potent inhibition of macrophage responses to IFN-gamma by live virulent Mycobacterium tuberculosis is independent of mature mycobacterial lipoproteins but dependent on TLR2. J Immunol *176*, 3019–3027. https://doi.org/10.4049/jimmunol.176.5.3019.
39. Pai, R.K., Convery, M., Hamilton, T.A., Boom, W.H., and Harding, C.V. (2003). Inhibition of IFN-gamma-induced class II transactivator expression by a 19-kDa lipoprotein from Mycobacterium tuberculosis: a potential mechanism for immune evasion. J Immunol *171*, 175–184. https://doi.org/10.4049/jimmunol.171.1.175.
40. Nagabhushanam, V., Solache, A., Ting, L.-M., Escaron, C.J., Zhang, J.Y., and Ernst, J.D. (2003). Innate inhibition of adaptive immunity: Mycobacterium tuberculosis-induced IL-6 inhibits macrophage responses to IFN-gamma. J Immunol *171*, 4750–4757. https://doi.org/10.4049/jimmunol.171.9.4750.
41. Kincaid, E.Z., and Ernst, J.D. (2003). Mycobacterium tuberculosis exerts gene-selective inhibition of transcriptional responses to IFN-gamma without inhibiting STAT1 function. J Immunol *171*, 2042–2049. https://doi.org/10.4049/jimmunol.171.4.2042.
42. Ting, L.M., Kim, A.C., Cattamanchi, A., and Ernst, J.D. (1999). Mycobacterium tuberculosis inhibits IFN-gamma transcriptional responses without inhibiting activation of STAT1. J Immunol *163*, 3898–3906.
43. Huang, L., Nazarova, E.V., Tan, S., Liu, Y., and Russell, D.G. (2018). Growth of Mycobacterium tuberculosis in vivo segregates with host macrophage metabolism and ontogeny. J Exp Med *215*, 1135–1152. https://doi.org/10.1084/jem.20172020.
44. Cohen, S.B., Gern, B.H., Delahaye, J.L., Adams, K.N., Plumlee, C.R., Winkler, J.K., Sherman, D.R., Gerner, M.Y., and Urdahl, K.B. (2018). Alveolar Macrophages Provide an Early Mycobacterium tuberculosis Niche and Initiate Dissemination. Cell Host Microbe *24*, 439-446.e4. https://doi.org/10.1016/j.chom.2018.08.001.
45. Rothchild, A.C., Olson, G.S., Nemeth, J., Amon, L.M., Mai, D., Gold, E.S., Diercks, A.H., and Aderem, A. (2019). Alveolar macrophages generate a noncanonical NRF2-driven transcriptional response to Mycobacterium tuberculosis in vivo. Sci Immunol *4*, eaaw6693. https://doi.org/10.1126/sciimmunol.aaw6693.
46. Zha, B.S., Desvignes, L., Fergus, T.J., Cornelius, A., Cheng, T.-Y., Moody, D.B., and Ernst, J.D. (2022). Bacterial Strain-Dependent Dissociation of Cell Recruitment and Cell-to-Cell Spread in Early M. tuberculosis Infection. mBio *13*, e0133222. https://doi.org/10.1128/mbio.01332-22.
47. Khader, S.A., Divangahi, M., Hanekom, W., Hill, P.C., Maeurer, M., Makar, K.W., Mayer-Barber, K.D., Mhlanga, M.M., Nemes, E., Schlesinger, L.S., et al. (2019). Targeting innate immunity for tuberculosis vaccination. J Clin Invest *129*, 3482–3491. https://doi.org/10.1172/JCI128877.
48. Cai, X., Zheng, W., Shi, X., Chen, L., Liu, Z., and Li, Z. (2018). HBx-Derived Constrained Peptides Inhibit the Secretion of Hepatitis B Virus Antigens. Mol Pharm *15*, 5646–5652. https://doi.org/10.1021/acs.molpharmaceut.8b00807.
49. Cai, X., Padilla, N.T., Rosbe, K., and Tugizov, S.M. (2024). Breast milk induces the differentiation of monocytes into macrophages, promoting human cytomegalovirus infection. J Virol *98*, e0117724. https://doi.org/10.1128/jvi.01177-24.
50. Srivastava, S., Grace, P.S., and Ernst, J.D. (2016). Antigen Export Reduces Antigen Presentation and Limits T Cell Control of M. tuberculosis. Cell Host Microbe *19*, 44–54. https://doi.org/10.1016/j.chom.2015.12.003.

Figures and figure legends

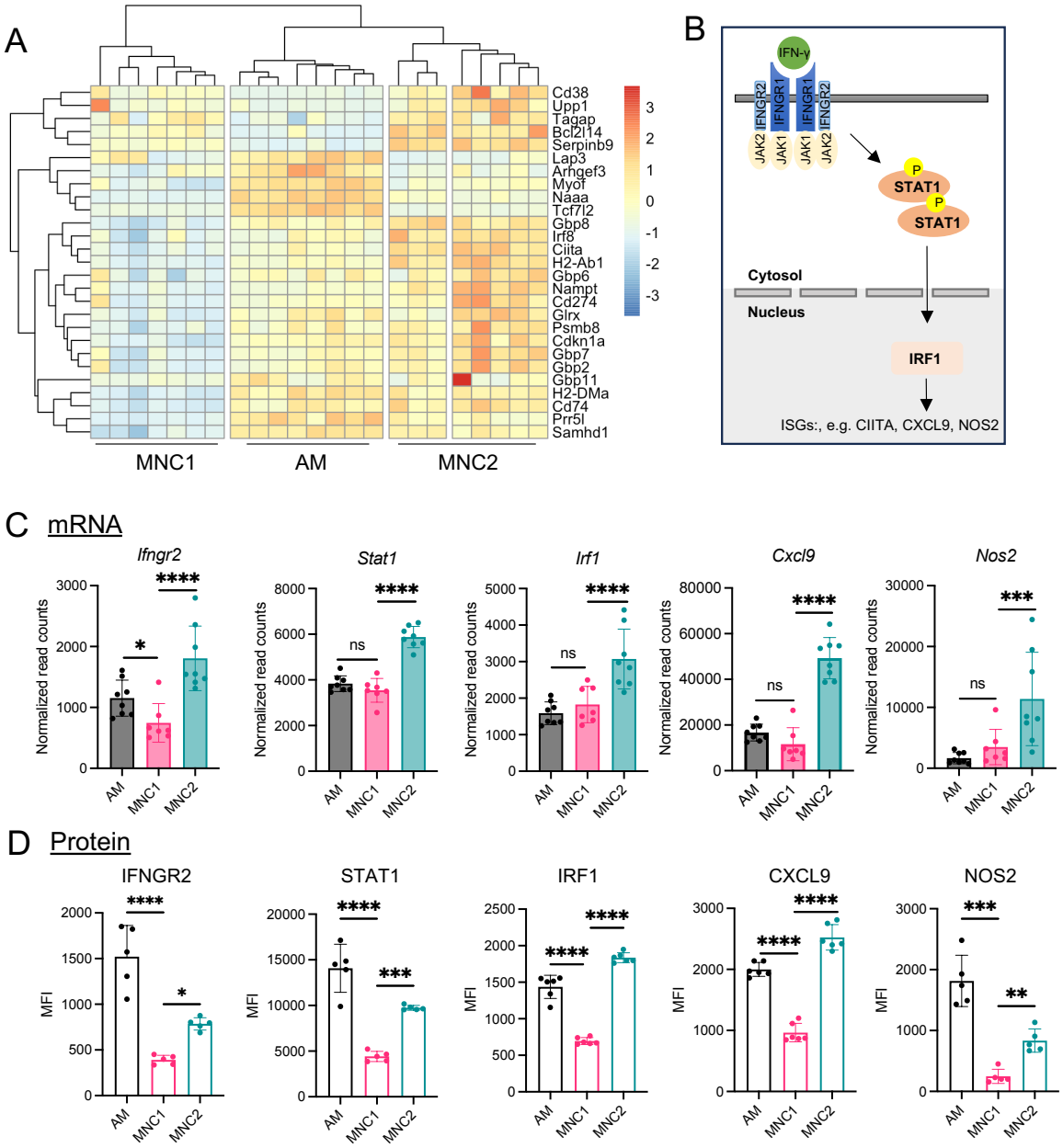

Fig 1. Key proteins in IFNγ signaling pathway are expressed at lower levels in MNC1.

(A) Analysis of RNA-seq dataset GSE288567 revealed that IFNγ signature genes are expressed at lower levels in MNC1 compared with AM and MNC2 (28 dpi). 10,000 live cells from each subset were sorted from the lungs of C57BL/6 mice infected with Mtb H37Rv-mCherry (n = 7-8).

(B) A schematic diagram shows the key signaling proteins regulating the response to IFNγ and representative IFNγ-responsive genes.

(C) Messenger RNAs encoding key signaling proteins regulating the response to IFNγ and representative IFNγ-responsive genes are differentially expressed in AM, MNC1, and MNC2. Shown are mRNA normalized read counts for different cell subsets (28 dpi) (n=7-8).

(D) Key signaling proteins regulating the response to IFNγ and protein products of representative IFNγ-responsive genes are differentially expressed in AM, MNC1, and MNC2. Flow cytometry was used to measure median fluorescent intensity (MFI) of proteins in different lung cell subsets from mice infected with H37Rv-ZsGreen (n=4-5).

Results are presented as mean ± SD. *p<0.05, **p<0.01, ***p<0.0001, ****p<0.0001 by Wald test via DESeq2 for (C) and one-way ANOVA for (D); ns = not significant.

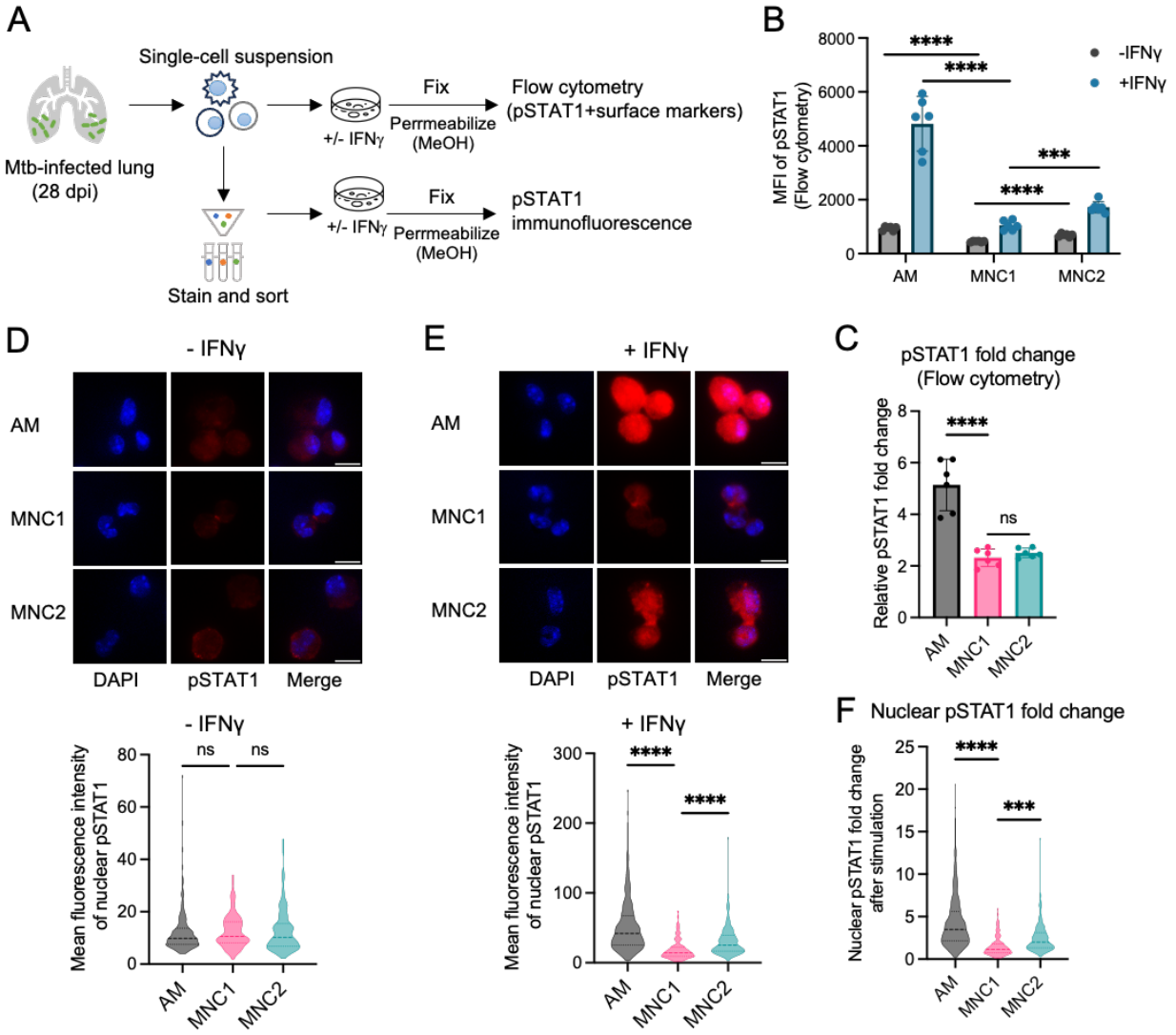

Figure 2. STAT1 phosphorylation is deficient in MNC1 treated with IFNγ ex vivo.

(A) Workflow for detecting pSTAT1 by flow cytometry and immunofluorescence. C57BL/6 mice were infected with Mtb H37Rv-ZsGreen via aerosol for 28 days. Lung single-cell suspensions were incubated with 20 ng/mL IFNγ for 15 min and subjected to pSTAT1 by flow cytometry analysis or immunofluorescence.

(B) MFI of pSTAT1 by flow cytometry for each lung cell subset in the absence or presence of IFNγ stimulation as described in panel A.

589 (C) Fold change of pSTAT1 MFI level by flow cytometry after cells were stimulated with IFNγ ex
590 vivo as described in panel B.

591 (D) Representative images of nuclear pSTAT1 immunofluorescence staining for each cell subset
592 sorted from Mtb-infected mice (28 dpi). Bottom panel shows the quantitation of mean fluorescence
593 intensity of nuclear pSTAT1 from n>145 cells.

594 (E) Representative images of nuclear pSTAT1 immunofluorescence staining for each cell subset
595 sorted from Mtb-infected mice (28 dpi) and stimulated with 20 ng/mL IFNγ for 15 min. The bottom
596 panel shows the quantitation of the mean fluorescence intensity of nuclear pSTAT1 from >155
597 cells.

598 (F) Fold change of nuclear pSTAT1 MFI by immunofluorescence staining after cells were
599 stimulated with IFNγ ex vivo as described in panel E.

600 Results are presented as mean ± SD. ***p<0.001, ****p<0.0001 by one-way ANOVA; ns = not
601 significant.

602

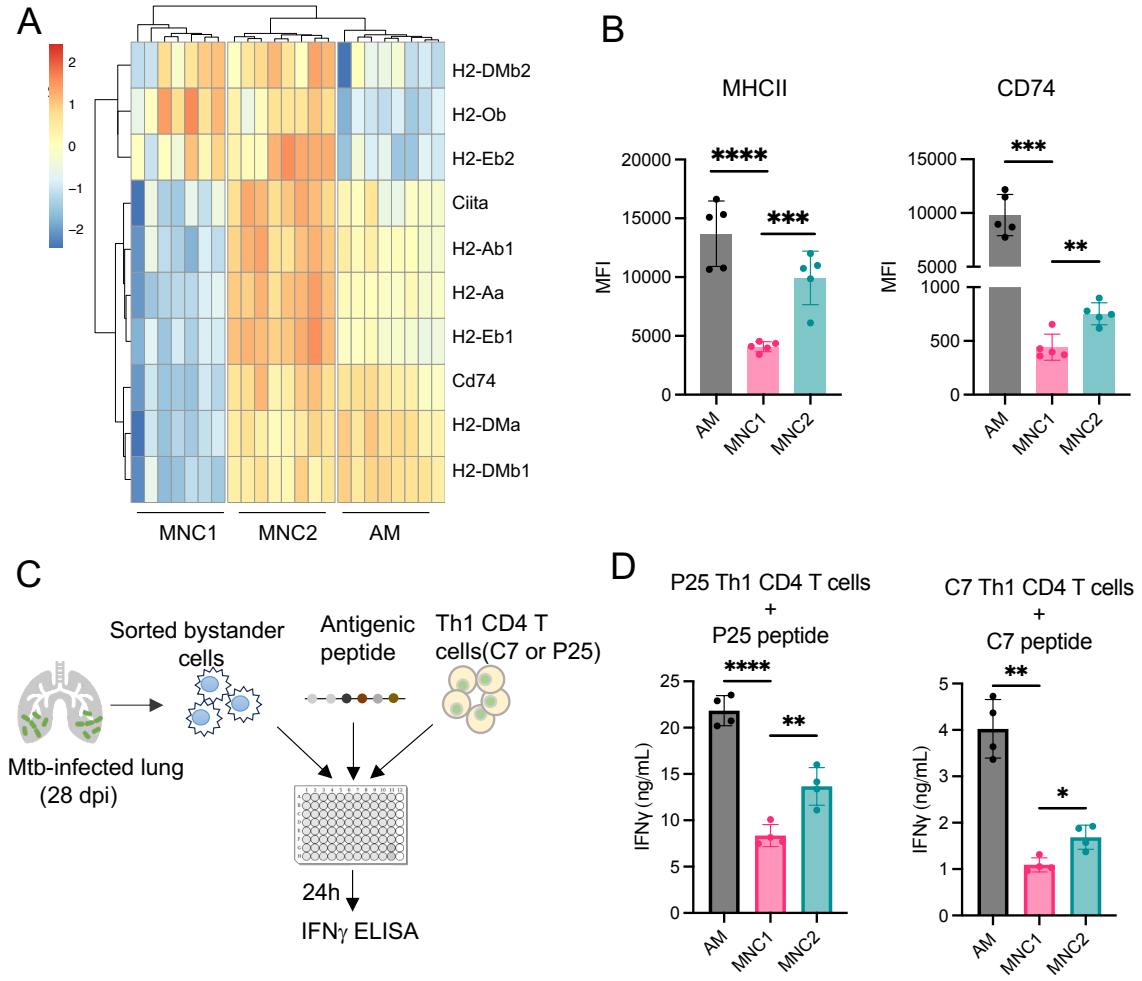

603

604 **Figure 3. Impaired responsiveness to IFNγ in MNC1 associates with defective MHC-II**
605 **antigen presentation.**

606 (A) Heatmap of the Z-scores from variance-stabilized read counts for genes related to MHC-II
607 antigen presentation (adjusted p-value ≤ 0.05 and |log2 fold change|>0.5).

608 (B) MNC1 express less surface MHC-II and CD74 than AM and MNC2. Flow cytometry was used
609 to measure MFI of MHC-II and CD74 in each cell subset from mice infected with Mtb H37Rv-
610 ZsGreen (28 dpi).

611 (C) Workflow of antigen-specific T cells and MNP co-culture. $1x10^4$ cells were sorted from mice
612 infected with Mtb H37Rv-ZsGreen and incubated with $2x10^5$ of the indicated Th1 polarized TCR
613 transgenic antigen-specific T cells and 10ug/mL antigenic peptide. After 24h, the supernatant was
614 filtered and assayed for IFNγ using ELISA.

615 (D) Impaired antigen presentation to CD4 T cells by MNC1. Supernatants were harvested from
616 the co-culture of antigen-specific T cells and different sorted cell subsets (n=4), and IFNγ level
617 was measured by ELISA.

618 Results are presented as mean ± SD. *p<0.05, **p<0.01, ****p<0.0001 by one-way ANOVA; ns
619 = not significant.

620

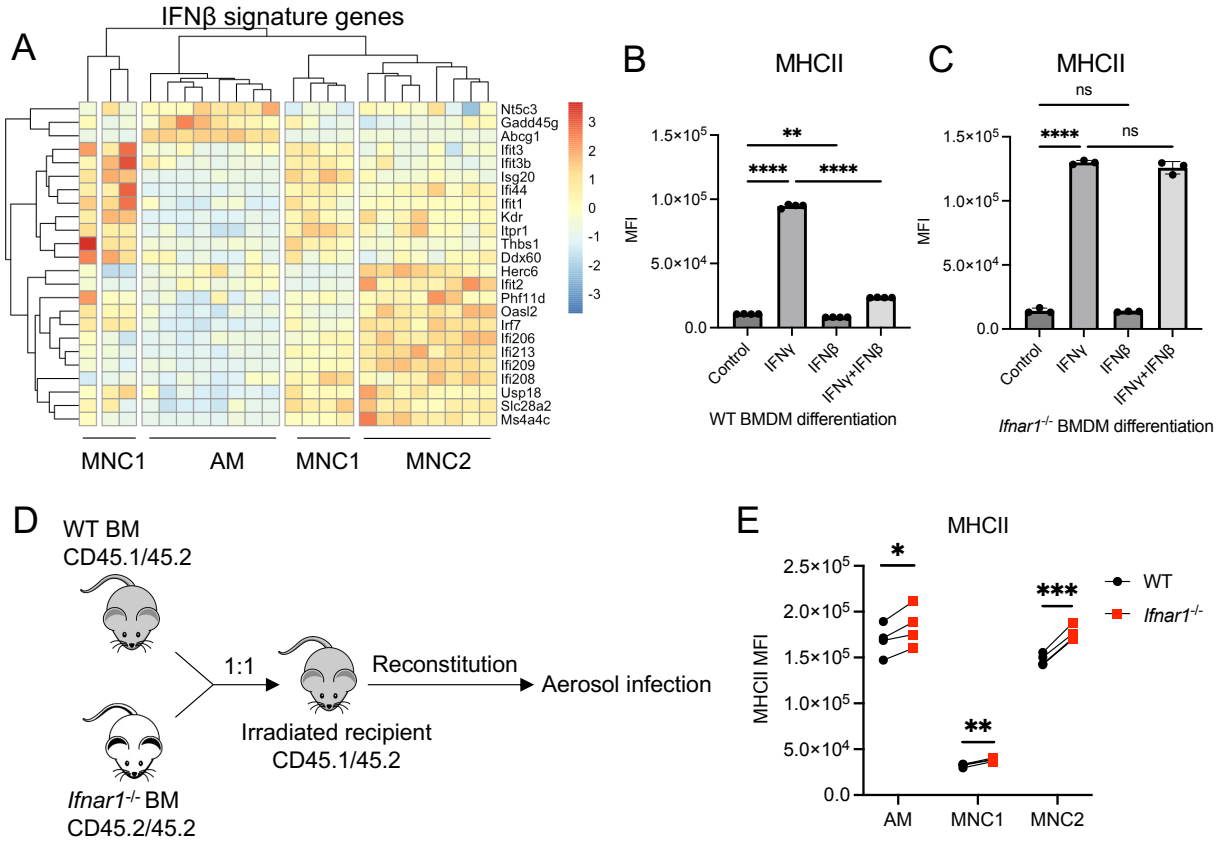

621

622 **Figure 4. Type I IFN contributes to defective IFNγ responses and MHC-II expression in**
623 **BMDM and MNP subsets.**

624 (A) Heatmap of the Z-scores from variance-stabilized read counts for IFNβ signature genes

625 (adjusted p-value ≤ 0.05 and |log2 fold change|>0.5).

(B-C) Type I IFN suppresses MHC-II expression induced by IFNγ in vitro. Wild-type (WT) or *Ifnar1*$^{-/-}$ bone marrow cells were differentiated in BMDM media containing the indicated interferon at 50 pg/mL for 6-7 days. The expression levels of MHC-II in BMDM were determined by flow cytometry and expressed as median fluorescence intensity (MFI).

(D) Experimental workflow. CD45.1/45.2 mice were irradiated and reconstituted with 1:1 mixed bone marrow from WT CD45.1/45.2 mice and *Ifnar1*$^{-/-}$ CD45.2/45.2 mice. After 6-week reconstitution, chimeras were aerosol challenged with Mtb H37Rv-ZsGreen.

(E) Type I IFN regulates MHC-II expression in AM, MNC1, and MNC2 in vivo. Flow cytometry was used to measure MHC-II MFI in each subset from WT: *Ifnar1*$^{-/-}$ mixed bone marrow chimeric mice infected with Mtb H37Rv-ZsGreen for 28 days (n=4).

Results are presented as mean ± SD. *p<0.05, **p<0.01, ***p<0.0001, ****p<0.0001 by one-way ANOVA for (B-C) or by paired t-test for (E); ns = not significant.

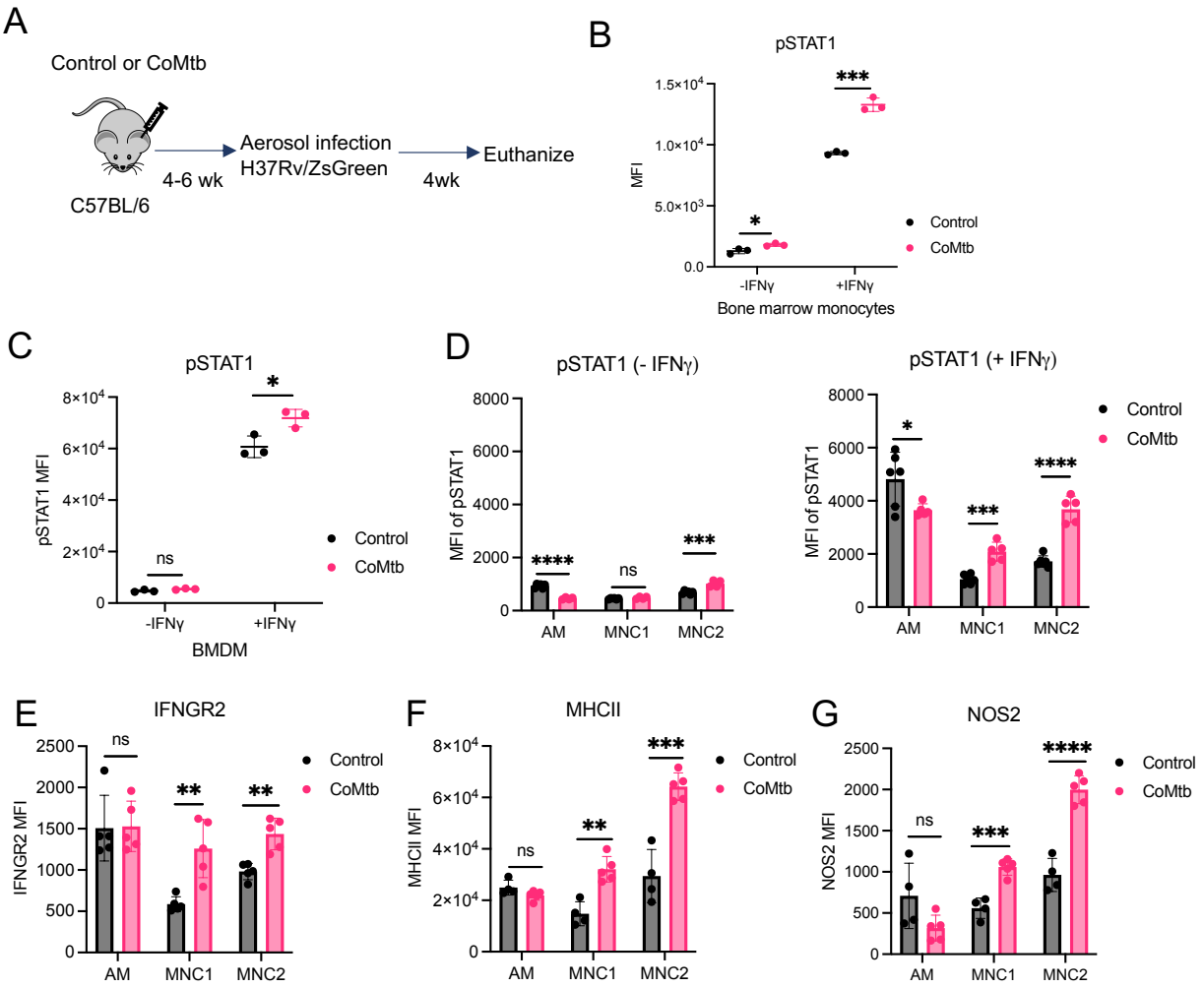

Figure 5. CoMtb improves IFNγ responsiveness of MNC but not AM.

(A) For the CoMtb studies, mice were inoculated intradermally in the ear with 10,000 CFU of Mtb H37Rv. After 4-6 weeks, control and CoMtb mice were infected with Mtb H37Rv-ZsGreen by aerosol and euthanized at 28 dpi.

644 (B) CoMtb increases IFNγ responsiveness in bone marrow monocytes. Bone marrow cells from
645 control or coMtb mice were stimulated with or without 20 ng/mL IFNγ for 15 min, followed by flow
646 cytometric measurement of pSTAT1 MFI (n=3).

647 (C) CoMtb increases IFNγ responsiveness in BMDM (n=3). Bone marrow cells from control or
648 coMtb mice were differentiated into BMDM for 6 days. Then BMDM were harvested and
649 stimulated with or without 20 ng/mL IFNγ for 15 min, followed by flow cytometric measurement of
650 pSTAT1 MFI (n=3)

651 (D) CoMtb improves IFNγ responsiveness in MNC1 and MNC2. Lung samples from control or
652 coMtb mice infected with H37Rv-ZsGreen by aerosol (28 dpi) were stimulated with or without 20
653 ng/mL IFNγ for 15 min, followed by flow cytometric measurement of pSTAT1 MFI (n=5-6).

654 (E) CoMtb increases expression of IFNGR2 in MNC1 and MNC2 (n=5-6). Shown are IFNGR2
655 MFI by flow cytometry for each lung cell subset from control or coMtb mice infected with H37Rv-
656 ZsGreen by aerosol (28 dpi).

657 (F) CoMtb enhances MHC-II expression in MNC1 and MNC2 (n=4). MHC-II MFI was measured
658 by flow cytometry (28 dpi).

659 (G) MNC1 and MNC2 from CoMtb mice show a higher expression of NOS2 by flow cytometry
660 (n=4) (28 dpi).

661 Results are presented as mean ± SD. *$p<0.05$, **$p<0.01$, ***$p<0.0001$, ****$p<0.0001$ by t-test; ns
662 = not significant.

663

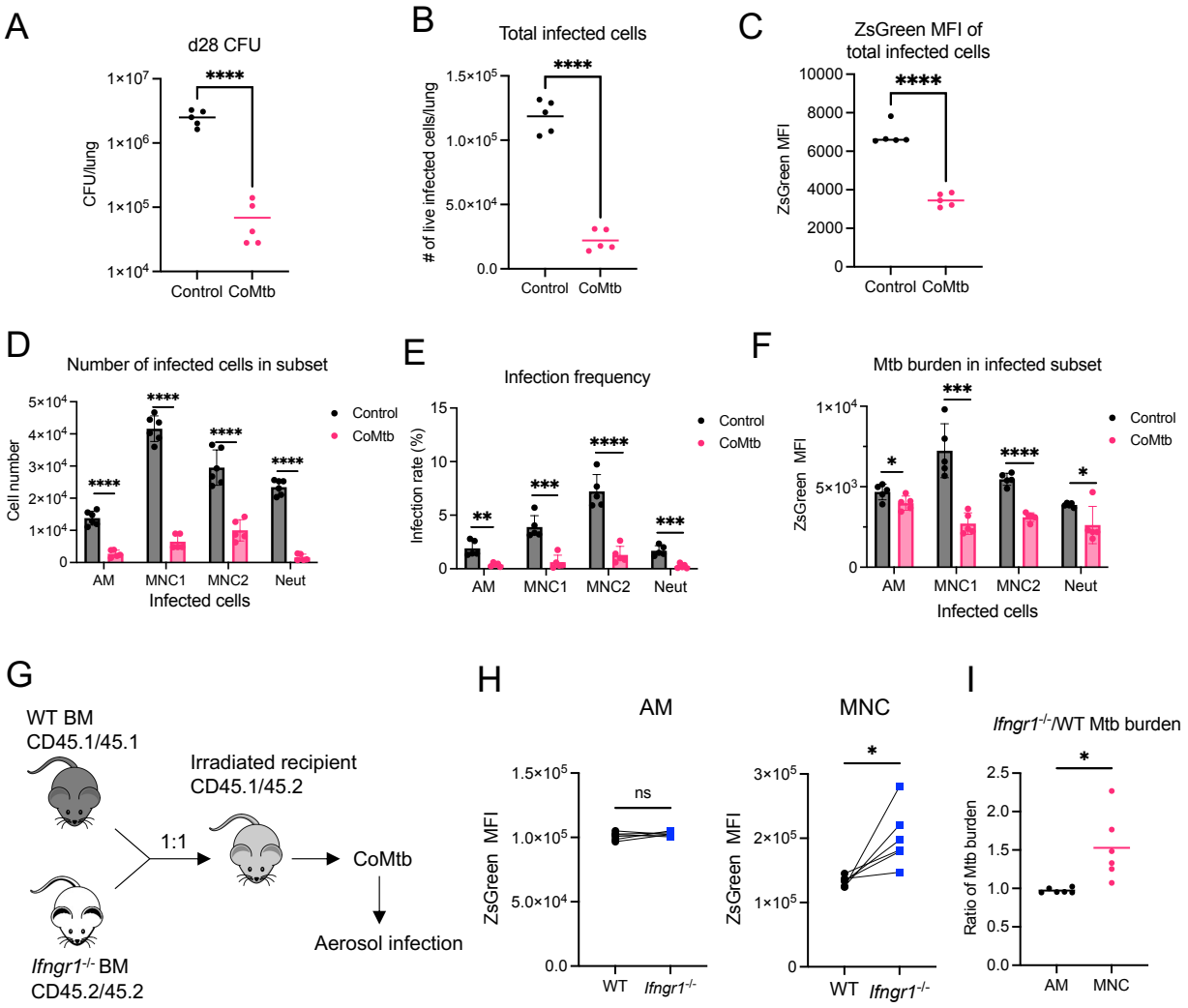

Figure 6. CoMtb-mediated prior immunity improves Mtb control in lung myeloid cells.

(A) Total lung CFU for control or CoMtb mice infected with Mtb H37Rv-ZsGreen via aerosol for 28 days (n=5).

(B) The number of total live infected cells from the same lung in panel A (n=5).

(C) Bacterial burden indicated by ZsGreen MFI by flow cytometry for total infected cells in panel B (n=5).

(D) Number of infected cells in each subset from the lungs of control and CoMtb mice infected with Mtb H37Rv-ZsGreen via aerosol for 28 days (n=5).

(E) Frequency of Mtb-infected cells in each lung subset from control and CoMtb mice infected with Mtb H37Rv-ZsGreen via aerosol for 28 days (n=5).

(F) Bacterial burden in each infected lung cell subset subset from control and CoMtb mice infected with Mtb H37Rv-ZsGreen via aerosol for 28 days (n=5).

(G) To generate mixed bone marrow chimeric mice, recipient (CD45.1/45.1) mice were irradiated and reconstituted with 1:1 mixed bone marrow from WT mice and *Ifngr1*$^{-/-}$ CD45.2/45.2 mice for 8 weeks. After 4 weeks of CoMtb, mice were aerosol challenged with Mtb H37Rv-ZsGreen.

680 (H) Bacterial burden indicated by ZsGreen MFI in infected AM and MNC cells from infected bone
681 marrow chimeric mice (n=6). There were insufficient infected MNC1 in CoMtb mice for separate
682 analyses, so MNC1 and MNC2 were combined as MNC in these studies.

683 (I) Ratio of *Ifngr1*$^{-/-}$/WT Mtb burden in different Mtb-infected subsets (ZsGreen^{+}) from infected
684 bone marrow chimeric mice (n=6).

685 Results are presented as mean ± SD. *p<0.05, **p<0.01, ***p<0.0001, ****p<0.0001 by unpaired
686 t-test for (A-E, I) or by paired t-test for (H); ns = not significant.

687